

**REPORT DOCUMENTATION PAGE**

*Form Approved*  
OMB No. 0704-01-0188

The public reporting burden for this collection of information is estimated to average 1 hour per response, including the time for reviewing instructions, searching existing data sources, gathering and maintaining the data needed, and completing and reviewing the collection of information. Send comments regarding this burden estimate or any other aspect of this collection of information, including suggestions for reducing the burden to Department of Defense, Washington Headquarters Services, Directorate for Information Operations and Reports (0704-0188), 1215 Jefferson Davis Highway, Suite 1204, Arlington VA 22202-4302. Respondents should be aware that notwithstanding any other provision of law, no person shall be subject to any penalty for failing to comply with a collection of information if it does not display a currently valid OMB control number.

**PLEASE DO NOT RETURN YOUR FORM TO THE ABOVE ADDRESS.**

DTIC COPY

1. REPORT DATE (DD-MM-YYYY) 07- 2007		2. REPORT TYPE REPRINT		3. DATES COVERED (From - To)	
4. TITLE AND SUBTITLE Formation of an F3 layer in the equatorial ionosphere: A result from Strong IMF changes				5a. CONTRACT NUMBER FA8718-06-C-0072	
				5b. GRANT NUMBER	
				5c. PROGRAM ELEMENT NUMBER 62101F	
6. AUTHORS V. V. Paznukhov, B. W. Reinisch, P. Song, X. Huang, T.W. Bullett*, and O. Veliz**				5d. PROJECT NUMBER 1010	
				5e. TASK NUMBER SD	
				5f. WORK UNIT NUMBER A1	
7. PERFORMING ORGANIZATION NAME(S) AND ADDRESS(ES) Center for Atmospheric Research, University of Massachusetts Lowell 600 Suffolk St. Lowell, MA				8. PERFORMING ORGANIZATION REPORT NUMBER  AFRL-RV-HA-TR-2008-1134	
9. SPONSORING/MONITORING AGENCY NAME(S) AND ADDRESS(ES) Air Force Research Laboratory/RVBXI 29 Randolph Road Hanscom AFB, MA 01731-3010				10. SPONSOR/MONITOR'S ACRONYM(S) AFRL/RVBXI	
				11. SPONSOR/MONITOR'S REPORT NUMBER(S)	
12. DISTRIBUTION/AVAILABILITY STATEMENT Approved for Public Release; distribution unlimited.					
13. SUPPLEMENTARY NOTES Reprinted from Journal of Atmospheric and Solar-Terrestrial Physics, Vol. 69, July 2007, pp. 1292-1304. © 2007 Elsevier Ltd. *Air Force Research Laboratory, RVBXI, Hanscom AFB, MA **Radio Observatorio de Jicamarca, Instituto Geofísico del Perú, Lima, Perú					
14. ABSTRACT We analyzed ionospheric observations made with digisondes in Jicamarca, Ramey, Wallops Island, Ascension Island, and Kwajalein Island during the major magnetic storm of November 9-10, 2004 that was associated with rapid interplanetary magnetic field (IMF) $B_z$ changes. The strongest ionospheric responses to the southward IMF $B_z$ turning were observed at the dip equator at Jicamarca where during the magnetic disturbance a dramatic F2 peak density depletion occurred around 1500 local time, accompanied by a fast upward motion of the plasma. In this process, an additional ionospheric layer, the F3 layer, formed with peak densities $NmF3$ exceeding $NmF2$ . This observation may be considered evidence of an equatorial plasma fountain enhancement caused by the magnetic field disturbance. Responses were observed in a large range of latitudes and local times. The best indicator of the responses appears to be the peak height of the F layer, since competing processes determine the peak densities. The observed responses at low latitude locations in the morning and dusk sectors pose challenges to the simple penetrating electric field model because the upward motion is inconsistent with the $E \times B$ drift associated with a dawn-dusk electric field. Clear responses in the Jicamarca local time sector occurred at latitudes as high as 28°, at Ramey, Puerto Rico. This latitude range appears to be beyond the range of the flux tube corresponding to the 900 km F3 layer peak height at Jicamarca, indicating a more extended uplifting of flux tubes.					
15. SUBJECT TERMS F3 layer      Equatorial plasma fountain      Electron density profiles      Digisonde      Space weather					
16. SECURITY CLASSIFICATION OF:			17. LIMITATION OF ABSTRACT	18. NUMBER OF PAGES	19a. NAME OF RESPONSIBLE PERSON
a. REPORT	b. ABSTRACT	c. THIS PAGE			Kenneth Walker
UNCL	UNCL	UNCL	UNL	30	19b. TELEPHONE NUMBER (Include area code)

Formation of an F3 layer in the equatorial ionosphere: A result from strong  
IMF changes

V. V. Paznukhov<sup>a,\*</sup>, B. W. Reinisch<sup>a</sup>, P. Song<sup>a</sup>, X. Huang<sup>a</sup>, T. W. Bullett<sup>b</sup>, O. Veliz<sup>c</sup>

<sup>a</sup> Center for Atmospheric Research, University of Massachusetts, 600 Suffolk Street,  
Lowell, MA, USA

<sup>b</sup> Air Force Research Laboratories, VSBXP, Hanscom AFB, MA, USA

<sup>c</sup> Radio Observatorio de Jicamarca, Instituto Geofisico del Peru, Lima, Peru

**Abstract**

THIS MATERIAL HAS BEEN CLASSIFIED  
FOR PUBLIC RELEASE BY CSO/PA  
17 Apr 07

We analyzed ionospheric observations made with digisondes in Jicamarca, Ramey, Wallops Island, Ascension Island, and Kwajalein Island during the major magnetic storm of November 9-10, 2004 that was associated with rapid interplanetary magnetic field (IMF) Bz changes. The strongest ionospheric responses to the southward IMF Bz turning were observed at the dip equator at Jicamarca where during the magnetic disturbance a dramatic F2 peak density depletion occurred around 1500 local time, accompanied by a fast upward motion of the plasma. In this process, an additional ionospheric layer, the F3 layer, formed with peak densities  $NmF3$  exceeding  $NmF2$ . This observation may be considered evidence of an equatorial plasma fountain enhancement caused by the magnetic field disturbance. Responses were observed in a large range of latitudes and local times. The best indicator of the responses appears to be the peak height

\* Corresponding author. Tel: 1 978 934 4913, fax: 1 978 459 7915

*E-mail address:* vadym\_paznukhov@uml.edu

20081229006

ESC 07 - 6100

DTIC COPY

of the F layer, since competing processes determine the peak densities. The observed responses at low latitude locations in the morning and dusk sectors pose challenges to the simple penetrating electric field model because the upward motion is inconsistent with the  $\mathbf{ExB}$  drift associated with a dawn-dusk electric field. Clear responses in the Jicamarca local time sector occurred at latitudes as high as  $28^\circ$ , at Ramey, Puerto Rico. This latitude range appears to be beyond the range of the flux tube corresponding to the 900 km F3 layer peak height at Jicamarca, indicating a more extended uplifting of flux tubes.

Keywords: F3 layer, Equatorial plasma fountain, Electron density profiles, Digisonde, Space weather

## 1. Introduction

Effects of geomagnetic storms on Earth's low and mid latitude ionosphere have long and intensively been studied (*e.g.*, Matsushita, 1959; Jones and Rishbeth, 1971; Kane, 1973; Mendillo, 1973; Proelss and Najita, 1975). Essentially, these studies established the complicated nature of the low and middle latitude ionosphere responses, but did not provide complete answers or a full understanding of the interaction mechanisms. For middle latitudes the general consensus is that following a storm sudden commencement the F2 layer critical frequency  $foF2$  first increases (positive phase) and then shows a long lasting (from a few hours up to a day) decrease (negative phase) typically with amplitudes larger than the initial increase. The equatorial ionosphere response is different, however. It is generally accepted that during storms the ionosphere at the equator often sees a weakly pronounced increase in  $foF2$ , which could be attributed to the decrease in the densities of the equatorial anomaly. It has also been suggested that

under certain conditions the electric field in the inner magnetosphere is capable of prompt penetration into the equatorial ionosphere (*e.g.*, Fejer et al., 1979; Gonzales et al., 1983). This topic has received much attention recently (*e.g.*, Basu et al., 2001), but more experimental evidence is needed in order to better understand this effect.

In this work we present a case study in which a strong magnetic storm associated with IMF changes resulted in a  $foF2$  decrease at the equator and the formation of an additional F layer above the F2 peak. Such layers have been reported for more than 50 years (*e.g.*, Sen, 1949), but they generally were attributed to atmospheric gravity waves that generate traveling ionospheric disturbances. It was not until the 1990's, however, that this phenomenon received sufficient attention and the nomenclature 'F3 layer' was introduced (*e.g.*, Balan et al., 1998) for the enhanced densities above the F2 layer. Topside sounders have also reported such topside stratifications (*e.g.*, Thampi et al., 2005). To date, the most consistent mechanism suggested to explain the F3 layer formation is the strengthening of the equatorial fountain (Balan et al., 1997) caused by the combination of the  $\text{ExB}$  plasma drift and neutral wind modulation.

In this study we make use of available digisonde observations at a number of stations at different latitudes and longitudes. Ionosondes are operated around the clock at all times and are therefore capable of monitoring the evolving ionospheric storm effects. Most digisondes included in this study made an ionogram every 15 minutes (except for Kwajalein Island where 5-min ionograms were available), a rate that is sufficient to describe the changes in the F region that result from IMF disturbances.

## **2. Data collection and analysis**

For the analysis of ionospheric responses to IMF changes we have selected the strong magnetic storm event of November 9-10, 2004 near the minimum of the solar sunspot cycle. During this storm the *Dst* index reached values  $< -200$  nT, and the *Ap* index peaked at 130. Figure 1 shows the interplanetary magnetic field (IMF) and solar wind data from the ACE satellite for the storm period, obtained from the ACE satellite Data-Center (<http://www.srl.caltech.edu/ACE/ASC/>). From the location of the ACE satellite and the measured solar wind speed we estimated the time required for this disturbance to arrive at Earth's magnetosphere in about 44 min, and accordingly shifted the solar wind data by this time in our plots. In the following discussion, we refer to the time-shifted solar wind data. The main period of interest is from 1900 to 2110 UT on November 9. During this time interval all solar wind parameters show strong variations, and the IMF *Bz* component turned negative reaching extremely low values of about  $-40$  nT while the solar wind speed and density both increased. Two hours later, *Bz* returned to zero and then changed to positive values of about the same magnitude.

Ionospheric data were obtained from selected stations of the digisonde network (<http://umlcar.uml.edu/stationlist>). Currently most of these instruments provide real-time data to the World Data Centers as well as to the University of Massachusetts Lowell Digital Ionosonde Data Base, DIDBase (Galkin et al., 1999). DIDBase archives contain ionograms together with the scaled data and allow for interactive editing of the data using the SAO-Explorer software package (<http://umlcar.uml.edu/SAO-X/>), which is convenient for analyses of ionograms. In this study we used DIDBase data records for the following locations: Jicamarca (GEO:  $12^{\circ}\text{S}$ ;  $283.2^{\circ}\text{E}$ ; GM:  $2.0^{\circ}\text{S}$ ,  $355.0^{\circ}\text{E}$ ;  $1^{\circ}$  dip), Ascension Island (GEO:  $8^{\circ}\text{S}$ ,  $346^{\circ}\text{E}$ ; GM:  $2.5^{\circ}\text{S}$ ,  $56.9^{\circ}\text{E}$ ;  $-16^{\circ}$  dip), Ramey (GEO:

18.5°N, 292.9°E; GM: 28.7°N, 5.0°E; 46.1° dip), Wallops Island (GEO: 37.9°N, 284.5°E; GM: 48.1°N, 355.5°E; 65.9° dip), and Kwajalein Island (GEO: 9.4°N, 167.4°E; GM: 4.0°N, 238.1°E; 8.9° dip). The Jicamarca, Ascension, and Kwajalein sites operated the advanced DPS-4 digisondes (Reinisch, 1996a), while Ramey and Wallops Island used the older Digisonde 256 (Reinisch, 1996b). Typically, the digisondes are programmed to make one ionogram every 15 minutes, or every 5 minutes during special campaigns. The scaling/analysis program ARTIST (Reinisch and Huang, 1983) scales each ionogram automatically in near real time, calculates the vertical electron density profile, and determines various ionospheric characteristics like the ionospheric F2 layer peak plasma frequency  $f_oF2$  and peak height  $hmF2$ . Test studies (Reinisch et al., 2005) have shown robustness and high precision of the ARTIST algorithm. Nonetheless, it is prudent to visually check the correctness of the automatic processing and to correct any errors that might occur. This is especially important for data collected under disturbed ionospheric conditions or in an electromagnetically noisy environment. Under certain conditions ionogram measurements cannot provide accurate vertical plasma density profiles, for example, in the case of high absorption in the D-layer that often occurs at higher latitudes or following prominent X-ray bursts, or during strong spread F conditions. The latter typically occur in the nighttime equatorial ionosphere when ionograms show strong spread echo returns that cannot be unambiguously inverted to electron density profiles, neither automatically nor manually. The Jicamarca electron density profile data in Figure 2 show the variations of the equatorial ionosphere, superimposed as white lines is the time-shifted IMF, scaled on the right. The top panel in Figure 2 is for the disturbed day of interest, November 9, 2004, and the bottom panel for a magnetically quiet day for

comparison. These "profilograms" give the electron density, with color-coding as indicated on the upper right side, as a function of height and time. For convenience, the time axis shows both universal time (UT) and local time (LT), with the sunset time marked by an arrow. The bottomside vertical profiles are calculated with the true height program NHPC (Huang and Reinisch, 2001), which calculates the electron density  $N_e(h)$  from the ionogram; the topside portion is an  $\alpha$ -Chapman extrapolation calculated with the Reinisch and Huang (2001) method. Ground-based ionosondes cannot measure the topside densities, and the typical Chapman distribution is likely not a good model during storm conditions, therefore one should consider some of the topside densities during the November 9 event only as a reference, as discussed in detail in the next section. Black squares mark  $hmF2$ , and triangles  $hmF3$ , *i.e.*, the peak heights of the F2 and F3 layers to be discussed in later sections. Compared to the quiet day, the noon peak densities on November 9 (before the storm onset) are ~25% higher and the peak height is slightly lower, but this is not a large variance. A fundamental change in the F region plasma distribution began at the time when Bz turned southward. The entire F2 layer displaced to higher altitudes and the peak density reduced by ~100%. No similar upward displacement occurred on the quiet day.

In Figure 3, the time sequence of November 9, 2004 ionograms recorded at Jicamarca between 1930-2130 UT (1430-1630 LT), provides a detailed look of the behavior of the F2 layer during the large swing of IMF Bz. Ionograms present the virtual heights  $h' = c \cdot t / 2$  (where  $c$  is the free-space speed of light and  $t$  is the echo travel time) of the ionospheric echoes as a function of frequency. In these ionograms, the colors indicate the measured Doppler frequencies, red indicating zero or very small Doppler

frequencies, and cyan indicating  $-4$  to  $-5$  Hz. The ionograms show only the O mode echoes (the X echoes have been removed from the display). The measured frequency shifts give an indication of the plasma velocity when transport dominates photochemical processes (Scali et al., 1997). Starting at around 1900 UT, the lower F2 layer plasma moved very slowly to larger heights keeping the Doppler frequencies close to zero. At 1930 UT, the echoes above 500 km ( $f > 10$  MHz) turned dark red (indicating  $\sim 2$  Hz Doppler frequency shift) and cyan near the F2 peak indicating large negative Doppler frequencies, which are typical for all F3 echoes in the next four ionograms. At 1945 UT the measured Doppler frequency shift at  $f > 8$  MHz is  $-5$  Hz, which corresponds to an apparent vertical plasma speed of more than 50 m/s. It is this upward streaming plasma that forms the F3 layer. From 1930 UT to 2030 UT the upper portion of the echo trace moves from 500 km to over 900 km (in terms of virtual range) supporting the concept of an upward plasma flow. From the sequence of Doppler signatures we conclude that the existence of an invisible F3 layer ( $NmF3 < NmF2$ ) before 1930 UT is unlikely. Notice that the apparent echo spread on the F3 trace at 1945 UT is not spread F, but is an artifact of the digital processing caused by signal saturation. The ionosonde cannot measure the electron densities above the F2 peak unless they become larger than  $NmF2$ , the peak density in the F2 layer. During the November 9 storm  $NmF2$  continued to decrease and the corresponding  $foF2$  value ( $foF2 [Hz] \approx 8.98 \sqrt{NmF2 [m^{-3}]}$ ) dropped from initially 14.0 MHz to 8.5 MHz at 1945 UT, and then to 6.5 MHz at 2030 UT (see also Figure 5 below), a reduction in density by a factor of  $\sim 5$ . The minimum virtual height,  $h'F3$ , of the F3 trace was 1060 km at this time, and increased to 1250 km at 2045 UT, which is close to the upper edge of the height range covered by the ionogram. The  $foF3$  at this time can

only be estimated as  $9.0 \pm 0.4$  MHz corresponding to a peak density of  $1.0 \times 10^{12} \text{ m}^{-3}$  (see also Figures 4 and 5). After 2045 UT  $foF2$  increased again, but no F3 layer trace showed on the ionograms, either because the echo trace was too high, *i.e.*, above 1300 km, or  $foF3$  has become smaller than  $foF2$ . The sporadic E layer (Es) at 100 km, likely associated with the equatorial electro jet, started developing at 1845 UT and reached plasma frequencies larger than 14 MHz at 2000 UT. The Es layer disappeared at 2115 UT, *i.e.*, at the time when Bz turned northward.

The evolving plasma redistribution is best illustrated by the sequence of vertical profiles calculated from the ionograms using a modified NHPC program that allows for an F3 layer. In Figure 4, the left panel shows the changing profiles from 1900 UT to 2030 UT during which time  $foF2$  was decreasing. At 1945 UT a ledge (inclination) occurred in the F region profile at  $\sim 360$  km, which we have identified as the remaining F2 peak, and above this height the F3 layer developed. The right panel gives the profiles from 2030 to 2200 UT (notice the change in the scale on the  $Ne$  axis). After 2015 UT the F3 layer peaked at higher altitudes but with decreasing densities, and the density of the F2 peak increased again, reaching its undisturbed value at  $\sim 2200$  UT. No topside profiles were plotted for 2100, 2115, and 2130 UT because of the uncertainties mentioned earlier. For the contour plot in Figure 2 we assumed that the topside densities at these times were equal to  $NmF2$  as indicated by the dashed lines in the right panel of Figure 4.

Part of the observed height and density changes can be related to typical diurnal variations. Figure 5 compares the measurements on November 9 with quiet day data around the event (the 19 quiet-days median for the period from October 20 to November 20). The error bars around the medians show the standard errors. The top panel of Figure

5 displays again the (time-shifted)  $B_z$  measurements for reference, the second and third panels show the densities and heights of the F layer peaks. Squares and triangles denote the F2 and F3 values, respectively. These plots confirm the slow upward motion of the F2 peak starting at 1900 UT on November 9 that was discussed earlier. The F2 peak reached a maximum height of 480 km at 2015 UT, close to the time when  $B_z$  reached its minimum. The F3 peak initially formed at 470 km, and by 2045 UT  $hmF3$  reached  $\sim 730$  km. Notice that  $NmF2$  decreased by a factor of  $\sim 5$  from 1900 to 2030 UT during which interval the quiet-day median value reduced by only 4%. The bottom panel shows the east-west component  $E_y$  of the electric field calculated from the plasma drift measured by the Jicamarca incoherent scatter radar (ISR) on November 9-10 and November 11-12, 2004. The  $E_y$  data were averaged over the height range of 405-510 km. During the southward turning of the IMF  $B_z$ , from 1900 to 2110 UT, the ionospheric electric field over Jicamarca became eastward, and  $E_y$  increased from 0 to 2.1 mV/m. This corresponds to a vertical plasma drift of  $\sim 95$  m/s, which is close to the  $\sim 110$  m/s velocity of the  $hmF3$  rise deduced from the ionogram profiles. The DPS-4 was not collecting drift data on this day.

Figures 6 - 9 compare the F2 peak heights and densities on November 9 with the quiet-day median values for several other low and mid-latitude digisonde stations. No F3 layers were observed at these locations. The Kwajalein digisonde was programmed to scan frequencies up to 15 MHz, corresponding to a peak density of  $2.8 \times 10^{12} \text{ m}^{-3}$ , a value that was exceeded around 2200 and 0000 UT. Ramey at  $28.7^\circ\text{N}$  GM (Figure 6) and Wallops Island at  $48.1^\circ\text{N}$  GM (Figure 7) are at nearly the same geomagnetic longitude as Jicamarca. On November 9 between 1900 UT and 2100 UT  $NmF2$  dropped at both

locations while  $hmF2$  increased slightly at Ramey, and fluctuated around the quiet day value at Wallops (blanketing Es prevented F layer measurements at 2030 and 2045 UT). A rapid increase in  $hmF2$  occurred at 2130 UT at Ramey and 2100 UT (or slightly earlier) at Wallops. These height changes coincided with the northward turning of IMF Bz.

The equatorial ionosphere at Kwajalein ( $4.0^{\circ}\text{N GM}$ ), as shown in Figure 8, was in the morning sector during the November 9 event, around 0630 LT, and exhibited a moderate increase in the F2 peak height starting at  $\sim 1930$  UT, but no unusual change in the peak density at the time when Bz turned negative. The ionograms (not shown here) did not indicate the development of an F3 layer, however, they indicate some restructuring of the vertical plasma distribution during the event. Two large  $NmF2$  peaks occurred later in the day after Bz had turned north (as mentioned above, the ionosonde frequency scan stopped at 15 MHz and could not measure the densities during these peaks). Another equatorial station, Ascension Island ( $2.5^{\circ}\text{S GM}$ ), was near the dusk terminator during the event at 1900 LT, and observed a steep increase in  $hmF2$  similar to Jicamarca, reaching a peak height of  $\sim 500$  km. Same as at Kwajalein, but unlike at Jicamarca, no F3 layer formed. The  $NmF2$  values decreased only slightly during the event at a similar rate as the quiet-day medians. At 2030 UT the peak density increased by a factor of  $\sim 2$  while  $hmF2$  returned to undisturbed values.

At higher latitudes, the Millstone Hill digisonde ( $52.9^{\circ}\text{N GM}$ ) observed reduced peak densities on November 9 compared to quiet days, but no clear effect of the large IMF Bz change was detected.

### 3. Summary and Discussion

Digisondes at equatorial and low and mid latitude stations measured the response of the ionosphere to the southward turning of the IMF Bz during the major magnetic storm of November 9, 2004. At Jicamarca, dayside equator, the IMF Bz southward turning caused a strong uplift of the F region plasma and the development of an F3 layer while the F2 peak density reduced by a factor of 5. The peak density  $NmF3$  observed during the event was about a factor of 2 smaller than  $NmF2$  before the IMF Bz turned southward. After the IMF turned back to northward again, the F3 layer disappeared, while the F2 layer electron density slowly recovered to the pre-event conditions within about one hour. An F3 layer was only observed at Jicamarca, and not at any of the other locations studied.

Comparing the observations at different stations, we conclude that the IMF-associated increase in the peak height is a common feature at low latitudes, while the peak densities vary from station to station. Table 1 summarizes the observations presenting the average peak densities and heights from three adjacent measurements at 2000, 2015 and 2030 UT. Peak values are given for the F2 and the F3 layer when the latter existed. The ratio of the peak height on the storm day to the quiet-day value is plotted in Figure 10 as a function of geomagnetic latitude. At different local times but at the equator, Kwajalein near the dawn terminator and Ascension near the dusk terminator, the normalized peak heights are  $\sim 1.3$ , compared with the dayside value of  $\sim 1.5$  at Jicamarca. The normalized peak height (dash-dot line) decreases away from the equator from  $\sim 1.5$  at Jicamarca to  $\sim 1.1$  at Ramey to  $\sim 1.0$  at Wallops Island. For comparison, Figure 10 also shows the normalized height (dashed line) of the flux tube that passes over

Jicamarca at a height of 900 km. If the rising of the F2 layer at different latitudes corresponds to the same field line, the peak heights at different stations should be around the given reference field line which gives the latitudinal extend of the equatorial rising flux tube. Clearly, in order to raise the F layer at  $\sim 28^\circ$ , the equatorial F layer had to be raised much higher.

The formation of the F3 layer has been suggested by Balan et al. (1997), based on numerical simulations, to be due to an enhanced equatorial plasma fountain effect, where the ionospheric plasma moves up at the equator and then distributes itself to higher latitudes. Greenspan et al. (1991), using DMSP measurements at 840 km altitude, suggested that a storm-induced eastward electric field causes an enhancement of the plasma fountain. The effect of the equatorial fountain enhancement is generally attributed to the development of an eastward electric field and an equatorward flow of the neutral wind. For the event of November 9, 2004 the Jicamarca ISR data also showed a strong eastward electric field that developed during the IMF Bz turning. Some authors attribute the development of an eastward electric field to the prompt penetration electric field (Greenspan et al., 1991; Foster and Rich, 1998; Huang et al., 2005). The penetrating electric field model can explain the observed correlation between southward turning of the IMF and the rising F layer observed at Jicamarca, as well as the formation of the F3 layer.

A puzzling fact in our observation is that the F-layer rose in a large range of local times. If the cause of these rises is the dawn-dusk electric field, then on the duskside and dawnside, at Ascension Island and Kwajalein, the  $E \times B$  drift should be in the azimuthal direction and not in the vertical direction, particularly at Ascension Island, which was on

the nightside of the terminator. The upward motion translates to a dusk-dawn electric field, opposite to the electric field coupled from the magnetosphere. Our observations may be explained by the local time dependence of photochemical processes (Spiro et al., 1988; Fejer et al., 1990).

The density change appears to be determined by a number of processes, such as photochemistry, transport, 3-D convection, and diffusion. The Jicamarca measurements may be most interesting for discussion of these processes. At the time when the F2 densities reach a minimum, the buildup of the F2 layer will set in. As Figure 5 suggests a significant density dip could be reached in a very short time. At this low density level, the production is larger than the recombination and the density starts building up with time. It takes between one and two hours for the ionosphere to reach its equilibrium. In this process, the photochemical imbalance produces an upward transport, but diffusion to higher altitudes, where the density is lower (above F layer peak), limits the build-up (Schunk and Nagy, 2000). In our observations enhanced upward convection was associated with the magnetic storm, and the steady state F2 layer moved up rapidly. The density within the upward moving flux tube decreased as the flux tube expanded, mostly because of the increase in length. The factor of 2 total decrease in the F3 layer peak density during the event can be understood as a result of this expansion. A field-aligned flow, by which plasma is deposited to the higher latitude ionosphere further reducing the equatorial density, may not be essential. At latitudes beyond the equatorial anomaly like at Ramey there was a tendency for decreased density, showing little evidence for plasma deposition from higher altitudes along the field lines. The reasons for the density decrease at high latitudes are not well understood.

## **Acknowledgement**

The UML authors were in part supported by AF contract F19628-02-C-0092. The Jicamarca Radio Observatory is a facility of the Instituto Geofisico del Peru and is operated with support from the NSF Cooperative Agreement ATM-0432565 through Cornell University. The authors wish to thank Dr. Chaosong Huang of MIT for helpful discussions and the UML undergraduate students K. Sorota and D. Khmyrov for their help in the ionogram data analysis.

## **References**

- Balan, N., Bailey, G. J., Abdu, M. A., Oyama, K. I., Richards, P. G., MacDougall, J., Batista, I. S., 1997. Equatorial plasma fountain and its effects over three locations: Evidence for an additional layer, the F<sub>3</sub> layer. *Journal of Geophysical Research* 102, 2047-2056.
- Balan, N., Batista, I. S., Abdu, M. A., MacDougall, J., Bailey, G. J., 1998. Physical mechanism and statistics of occurrence of an additional layer in the equatorial ionosphere. *Journal of Geophysical Research* 103, 29169-29182.
- Basu, Su., Basu, S., Valladares, C. E., Yeh, H.-C., Su, S.-Y., MacKenzie, E., Sultan, P. J., Aarons, J., Rich, F. J., Doherty, P., Groves, K. M., Bullett, T. W., 2001. Ionospheric effects of major magnetic storms during the international space weather period of September and October 1999: GPS observations, VHF/UHF scintillations, and in situ density structures at middle and equatorial latitudes. *Journal of Geophysical Research* 106, 30389-30414.

- Fejer, B. G., Gonzales, C. A., Farley, D. T., Kelley, M. C., Woodman, R. F., 1979. Equatorial electric fields during magnetically disturbed conditions 1. The effect of the interplanetary magnetic field. *Journal of Geophysical Research* 84, 5797-5802.
- Fejer, B. G., R. W. Spiro, R. A. Wold, and J. C. Foster, 1990. Latitudinal variations of penetration electric fields during magnetically disturbed periods: 1986 SUNDIAL observations and model results, *Annales Geophysicae* 8, 441-454.
- Foster, J. C., Rich, F. J., 1998. Prompt midlatitude electric field effects during severe geomagnetic storms. *Journal of Geophysical Research* 103, 26367-26372.
- Galkin, I. A., Kitrosser, D. F., Kecic, Z., Reinisch, B. W., 1999. Internet access to ionosondes, *Journal of Atmospheric and Solar-Terrestrial Physics* 61, 181-186.
- Gonzales, C. A., Behnke, R. A., Kelley, M. C., Vickrey, J. F., Wand, R., Holt, J., 1983. On the longitudinal variations of the ionospheric electric field during magnetospheric disturbances. *Journal of Geophysical Research* 88, 9135-9144.
- Greenspan, M. E., Rasmussen, C. E., Burke, W. J., Abdu, M. A., 1991. Equatorial density depletions observed at 840 km during the great magnetic storm of March 1989. *Journal of Geophysical Research* 96, 13931-13942.
- Huang, C.-S., Foster, J. C., Kelley, M. C., 2005. Long-duration penetration of the interplanetary electric field to the low-latitude ionosphere during the main phase of magnetic storms. *Journal of Geophysical Research* 110, A11309, doi:10.1029/2005JA011202.
- Huang, X., Reinisch, B. W., 2001. Vertical electron content from ionograms in real time, *Radio Science* 36, 335-342.

- Jones, K. L., Rishbeth, H., 1971. The origin of storm increases of mid-latitude F-layer electron concentration. *Journal of Atmospheric and Terrestrial Physics* 33, 391-401.
- Kane, R. P., 1973. Global evolution of F2 region storms. *Journal of Atmospheric and Terrestrial Physics* 35, 1953-1966.
- Matsushita, S., 1959. A Study of the Morphology of Ionospheric Storms. *Journal of Geophysical Research* 64, 305-321.
- Mendillo, M., 1973. A study of the relationship between geomagnetic storms and ionospheric disturbances at mid-latitudes. *Planetary and Space Science* 21, 349-358.
- Proelss, G. W., Najita, K., 1975. Magnetic storm associated changes in the electron content at low latitudes. *Journal of Atmospheric and Terrestrial Physics* 37, 635-643.
- Reinisch, B. W., Huang, X., 1983. Automatic calculation of electron density profiles from digital ionograms, 3, Processing of bottomside ionograms. *Radio Science* 18, 477-492.
- Reinisch, B. W., 1996a. Ionosonde. In: Dieminger, W., Hartmann, G. K., Leitinger, R. (Eds.), *Upper Atmosphere*, Springer, Berlin, pp. 370-381.
- Reinisch, B. W., 1996b. Modern Ionosondes. In: Kohl, H., Rüster, R., Schlegel, K. (Eds.), *Modern Ionospheric Science*. European Geophysical Society, 37191 Katlenburg-Lindau, Germany, pp. 440-458.
- Reinisch, B. W., Huang, X., 2001. Deducing topside profiles and total electron content from bottomside ionograms. *Advances in Space Research* 27, 23-30.
- Reinisch, B. W., Huang, X., Galkin, I. A., Paznukhov, V., Kozlov, A., 2005. Recent advances in real-time analysis of ionograms and ionospheric drift measurements with digisondes. *Journal of Atmospheric and Solar-Terrestrial Physics* 67, 1054-1062.

- Scali, J. L., Reinisch, B. W., Kelley, M. C., Miller, C. A., Swartz, W. E., Zhou, Q. H., Radicella, S., 1997. Incoherent scatter radar and digisonde observations at tropical latitudes, including conjugate point studies. *Journal of Geophysical Research* 102, 7357-7367.
- Schunk, R. W., Nagy A. F., 2000, *Ionospheres*, Cambridge Univ. Press, Cambridge.
- Sen, H. Y., 1949. Stratification of the F2-layer of the Ionosphere Over Singapore. *Journal of Geophysical Research* 54, 363-366.
- Spiro, R. W., Wolf, R. A., Fejer, B. G., 1988. Penetrating of high-latitude-electric-field effects to low latitudes during SUNDIAL 1984. *Annales Geophysicae* 6, 39-49.
- Thampi, S. V., Ravindran, S., Devasia, C. V., Pant, T. K., Sreelatha, P., Sridharan, R., 2005. First observation of topside ionization ledges using radio beacon measurements from low Earth orbiting satellites, *Geophysical Research Letters* 32, L11104, doi:10.1029/2005GL022883.

## FIGURE CAPTIONS

Figure 1. Geosynchronous H-component, solar wind ion density and velocity, and the IMF measured on the ACE satellite for a period of the major magnetic storm on November 9-10, 2004. The ACE data have been shifted by 44 min to take account of the solar wind convection time.

Figure 2. Digisonde profilograms with color-coded densities for Jicamarca with the IMF Bz data superimposed; November 9-10, 2004 in the top panel, a quiet day, October 27-28, 2004 in the bottom panel. The layer peak heights are marked by squares for the F2 layer, and triangles for the F3 layer. The magnetic field data, scaled on the right, are time-shifted to account for the ACE satellite location.

Figure 3. Ionogram sequence at Jicamarca show the development of the F3 layer and the depletion of the electron density in the F2 layer during the observed IMF Bz changes. The color of the O-mode echoes indicates the measured Doppler frequencies according to the legend on the upper right, all X-mode echoes have been digitally removed from the ionograms.

Figure 4. Electron density profiles at Jicamarca show the density depletion in the F2 layer and the appearance of the F3 layer following the southward turning of the IMF Bz. For the profiles from 2100 UT to 2130 UT the topside parts are not shown because of the uncertainties in estimating the topside profiles.

Figure 5. The top panel shows the time-shifted  $B_z$  data on November 9-10, 2004. The second and third panels display the F2 and F3 layer peak densities and heights at Jicamarca. Squares and triangles indicate F2 and F3 values, respectively, on November 9-10, while the thin lines with circles represent the quiet-day median data. The error bars represent standard errors. The bottom panel shows the east-west component  $E_y$  of the electric field measured by the Jicamarca incoherent scatter radar on November 9-10 and November 11-12 (quiet day).

Figure 6. The F2 layer peak densities and heights at Ramey on November 9-10, 2004, in the same format as the two lower panels in Figure 5.

Figure 7. Wallops Island data for November 9-10, 2004, in the same format as Figure 6.

Figure 8. Kwajalein data on November 9-10, 2004, in the same format as Figure 6.

Figure 9. Ascension data on November 9-10, 2004, in the same format as Figure 6.

Figure 10. Ratio of ionosphere peak height during the disturbance to the quiet-day peak height values as a function of geomagnetic latitude (dash-dotted line). For each location three values measured at 2000, 2015 and 2030 were averaged. The dashed line shows the normalized heights of the magnetic field line passing over Jicamarca at 900 km.

## TABLE CAPTIONS

Table 1. Station GM coordinates and peak characteristics of the ionospheric response.

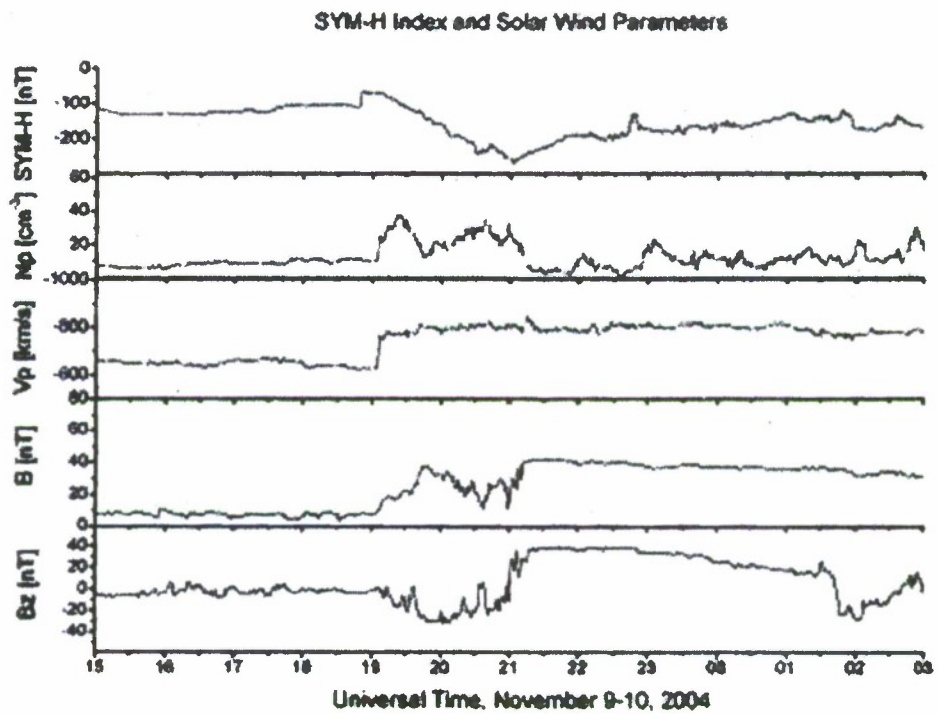


Figure 1

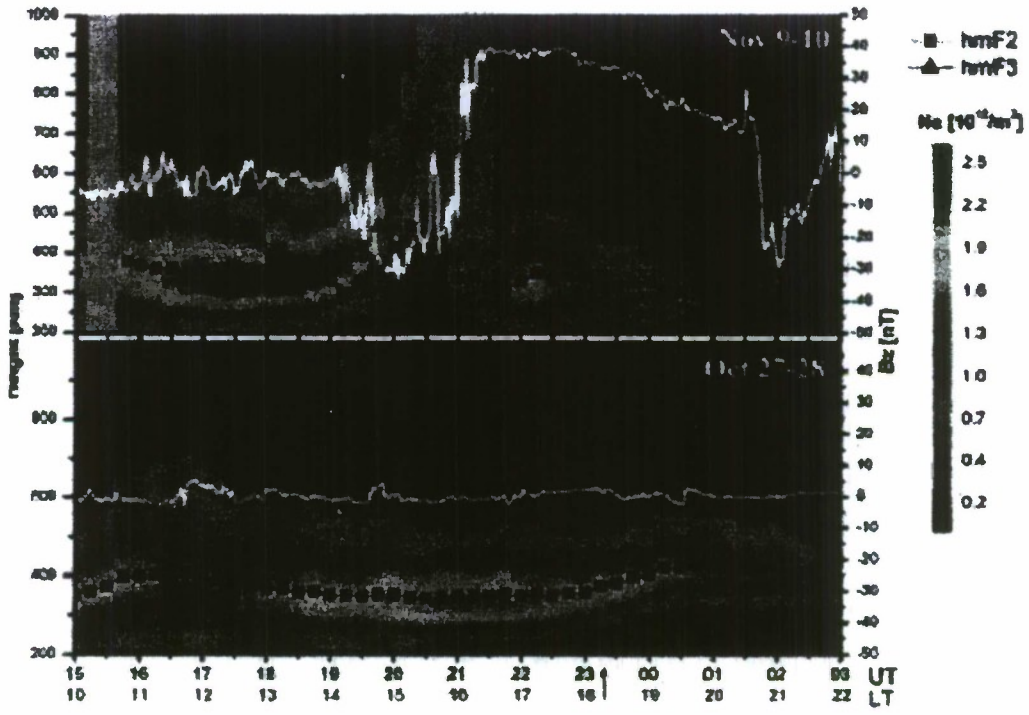


Figure 2

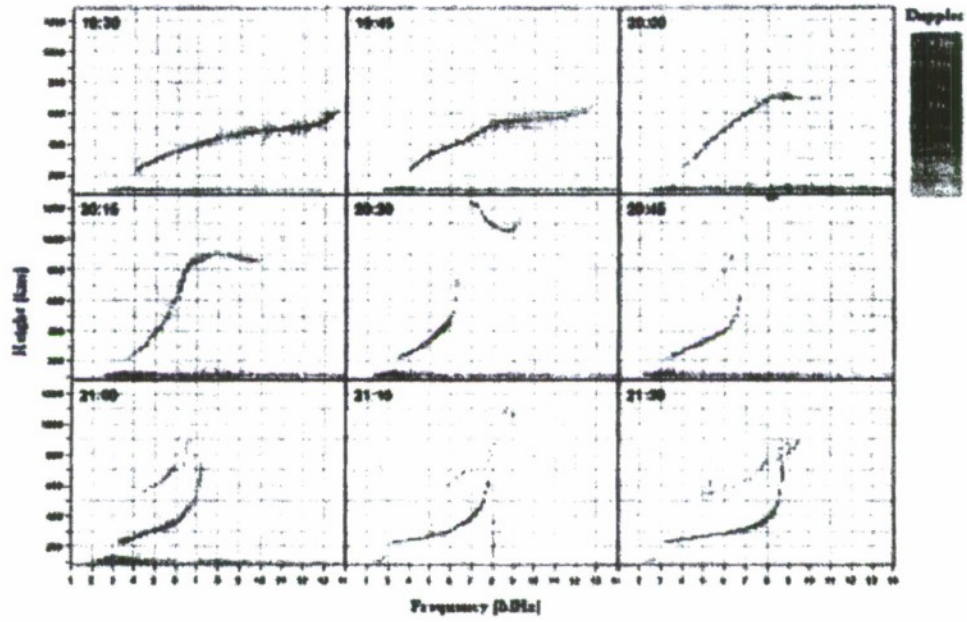


Figure 3

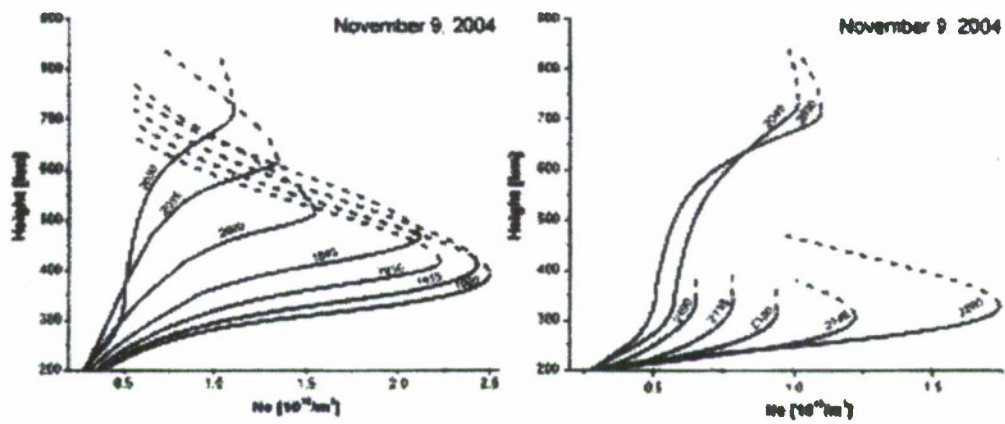


Figure 4

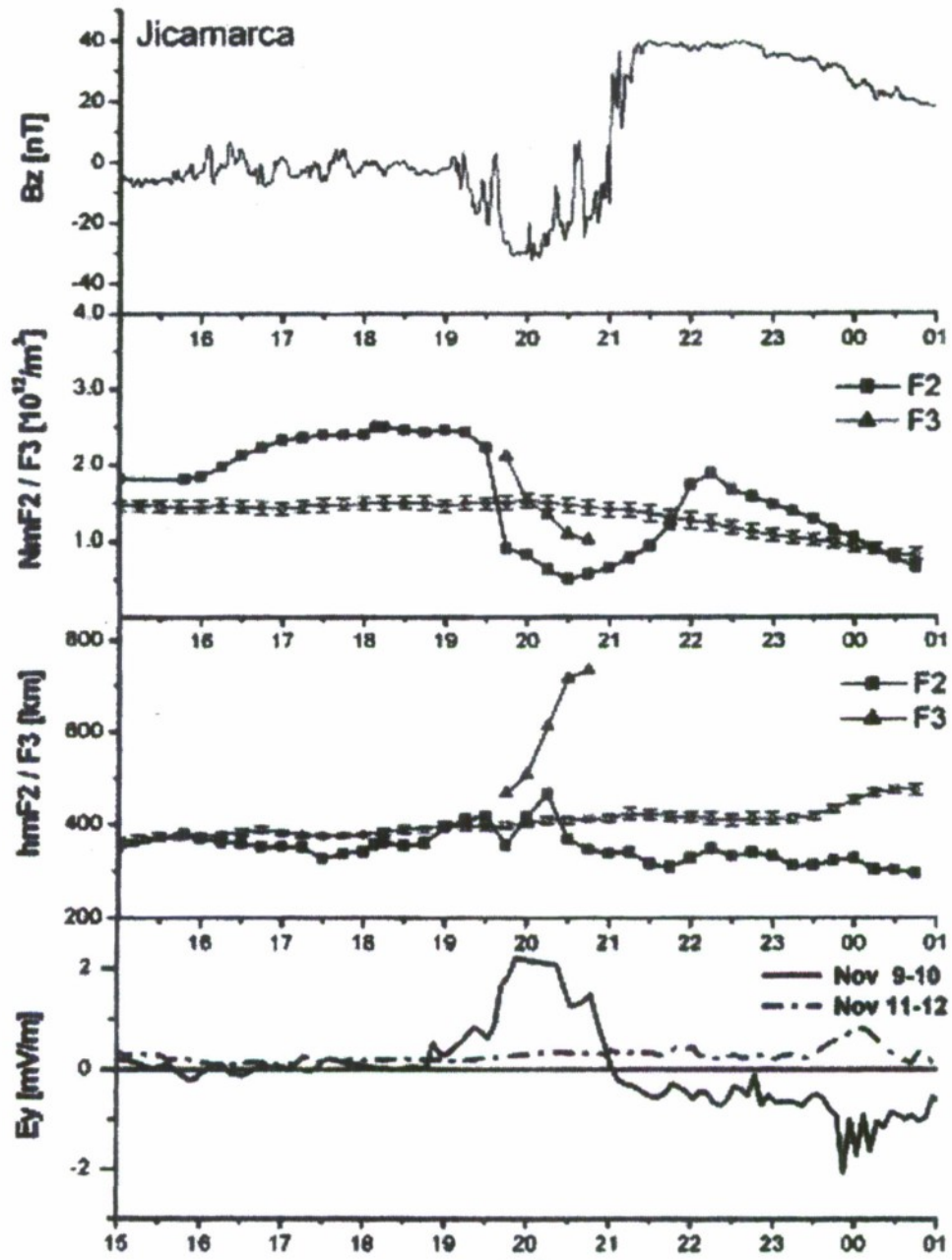


Figure 5

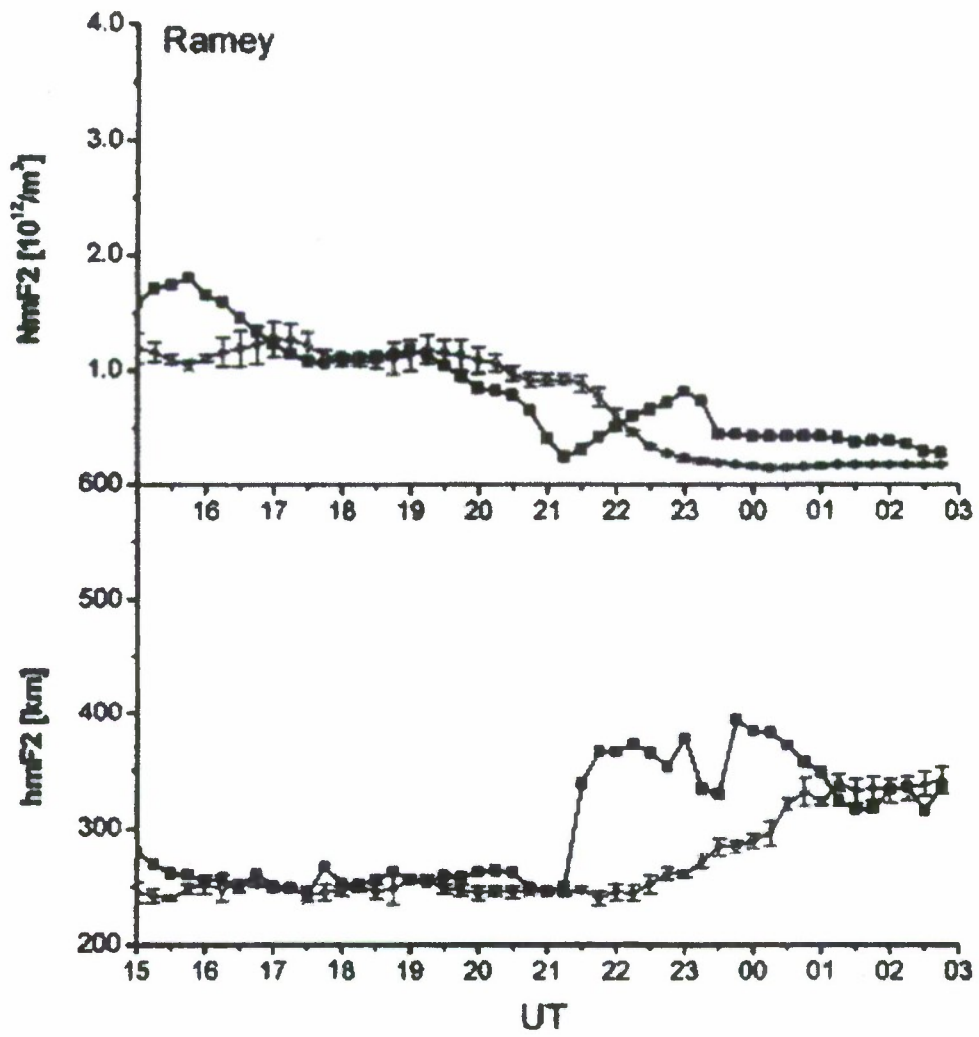


Figure 6

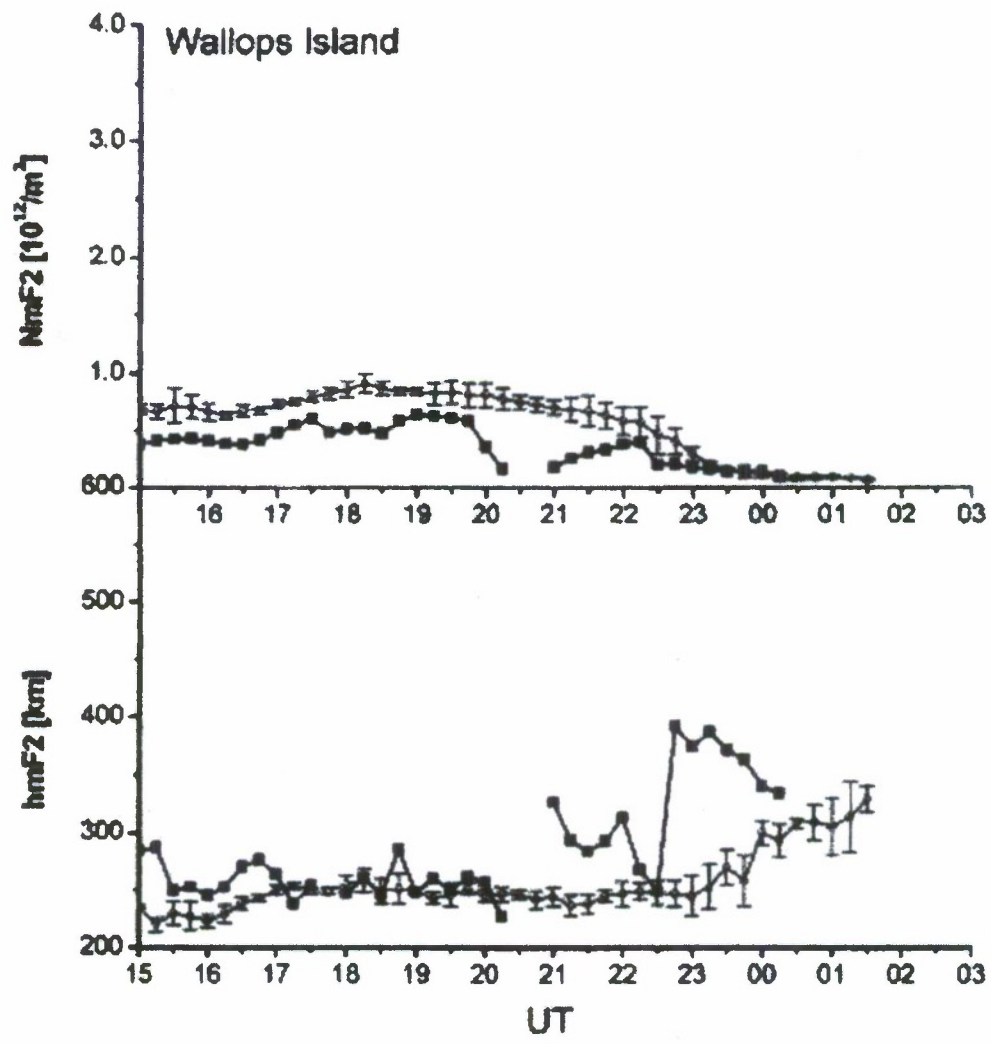


Figure 7

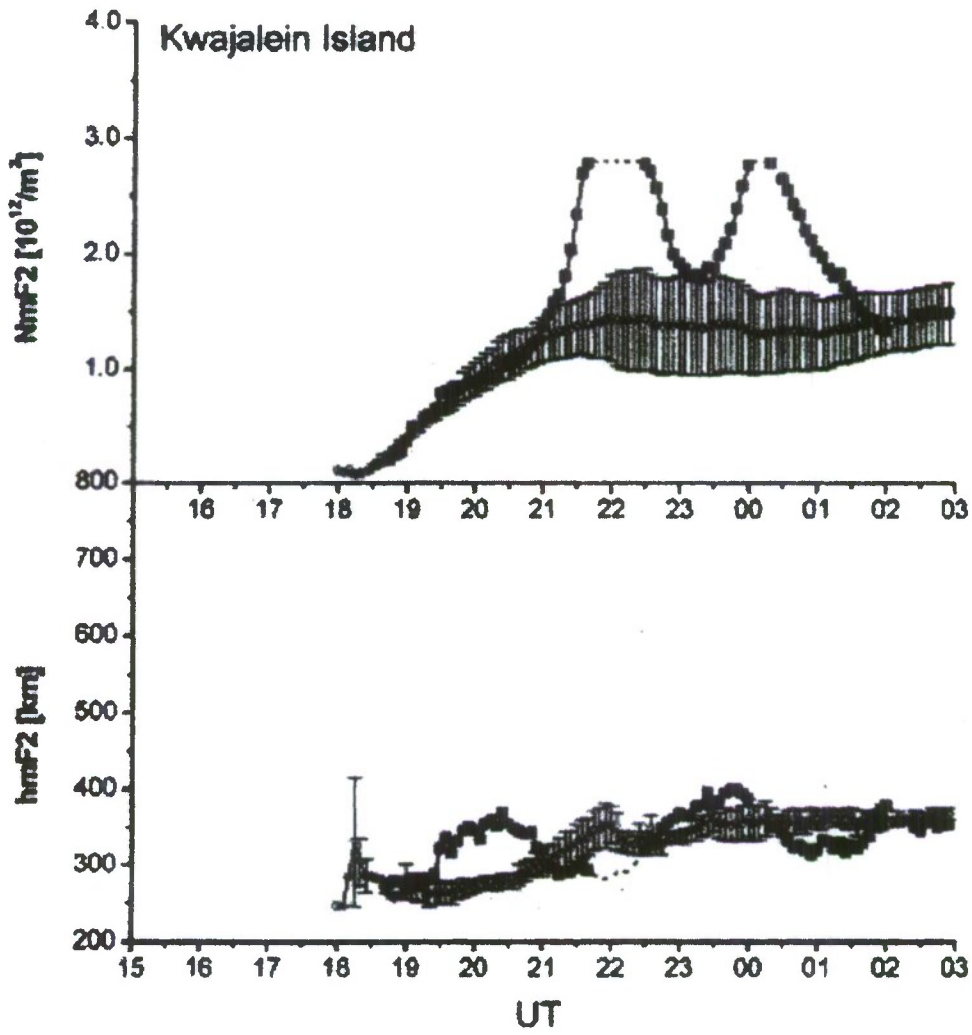


Figure 8

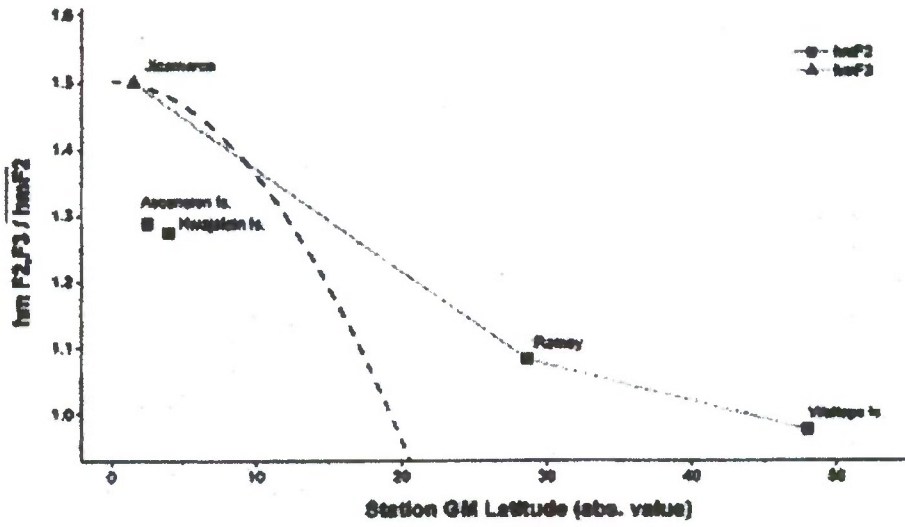


Figure 10

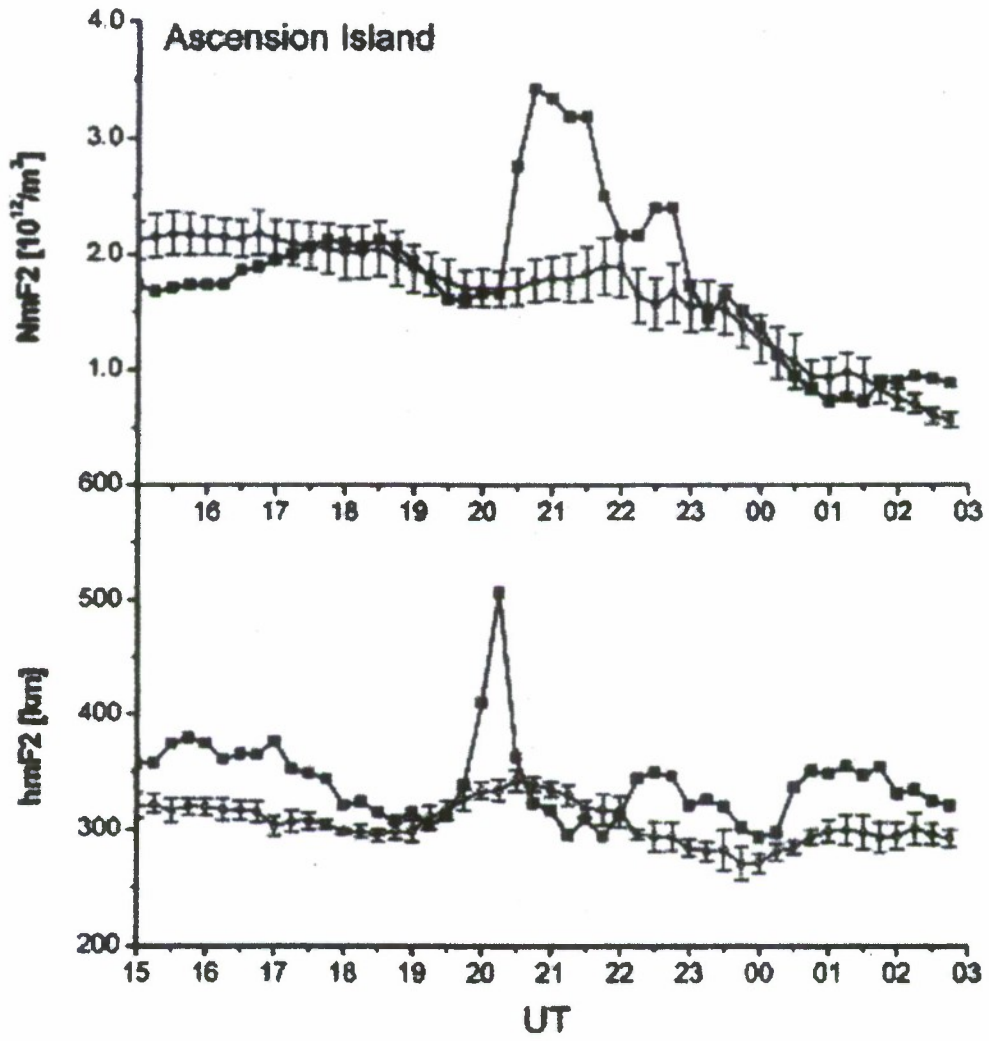


Figure 9